Influence of Channel and Yoke Design and Clogging on Turbulent Flow and Heat Exchange in Induction Channel Furnaces

JAKOVICS Andris[1], PAVLOVS Sergejs[1], BOSNYAKS Dmitrijs[1], SPITANS Sergejs[1], BAAKE Egbert[2], NACKE Bernard[2]

(1. Laboratory for Mathematical Modelling of Environmental and Technological Processes, University of Latvia, 8 Zellu str., LV-1002, Riga, Latvia;
2. Institute of Electrotechnology, Leibniz University of Hannover, Wilhelm-Busch-Str. 4, D-30167 Hannover, Germany)

Abstract: Low frequency oscillations of temperature field in the industrial induction channel furnace (ICF) with symmetrical and widened channel branches as well as different iron yoke positions are obtained using Large Eddy Simulation (LES) approach. The application of *k-ω* Shear Stress Transport (SST) turbulence model for computations of ICF with typical clogging shapes shows their influence on temperature and induced Joule heat power distributions, which are to be precise in LES study.
Key words: ICF; LES; SST; low-frequency oscillations; channel and throat clogging.

ICF, the industrial metallurgical equipment with high electrical and thermal efficiency, is used for melting, holding and casting of metals and alloys. Damages like erosion, clogging and infiltration of the ceramic lining in the channel as well as local overheating in the channel may lower the cleanness of the processed melt as well as the effectiveness and safety of ICF operation. The way to minimize these known problems is the variation of ICF parameters for choice of ICF operation regimes, which provide controlled intensification of turbulent heat exchange between the channel and the throat.

1 Computed Models of ICF

For long-term LES study of heat and mass exchange in the melt the following models of ICF (induced power in the melt ~ 215 kW) are chosen [1–3], whose geometries are variations of the Model (a) original design [2]:

√ *Model (a)* with two symmetric channel branches (**Tab. 1**(a)) – channel loop's external radius – 0.4 m; channel cross-section's smaller radius – 0.06 m:

√ *Model (b)* with widened channel branch (Tab. 1(b));

√ *Model (c)*, the modification of the model (b), which moved iron yoke (Tab. 1(c)).

Table 1 Variations of ICF original model

	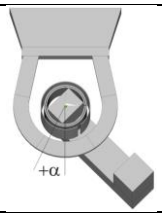	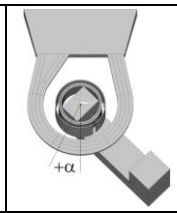	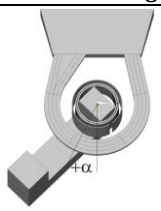			
Original design of ICF *(above)* as well as its variations *(right)*	(a)	(b)	(c)	(d)	(e)	(f)
Channel branches	symmetrical	widened (200%)	widened (200%)	narrowed (50%)	symmetrical	symmetrical
Iron yoke of inductor	α = -45º	α = -45º	α = 45º	α = 45º	α = 45º	α = 45º
Non-conductive sediments' shape	–	–	–	build-up in left channel branch	"hill" at throat bottom	"wall" at throat bottom
Inductor current amplitude [A]	1075	1865	1850	1850	1850	1850
Flow time t [s]	0–700	0–200	0–200	–	–	–
Model of turbulence	3D LES			3D *k-ω* SST		

For SST computations of non-conductive sediments' influence on velocity and temperature field the following ICF models (inductor amplitude current – 1850 A, number of turns – 28) are chosen:

√ *Model (d)* with narrowed channel branch (Tab. 1(d)), which simulates build-up in the channel;

√ *Model (e)* and *Model (f)* with sediments at the throat bottom in form of "hill" and "bank" (Tab. 1(e), (f)).

2 Temperature Maximum and Its Position in ICF Channel

The obtained results for long-term oscillations of temperature maximum in the channel T_{max} and its position α for models (a), (b), (c) are shown in **Fig. 1** and **Tab. 2**. To retrace, the detailed discussion of computational results for temperature fields and melt flow structure for models (a), (b) is provided in [1–3].

The comparison of results for model (c), which combines two non-symmetrical factors (channel branch widening and iron yoke position changing) in one (the left) channel branch, with model (b) show the following:

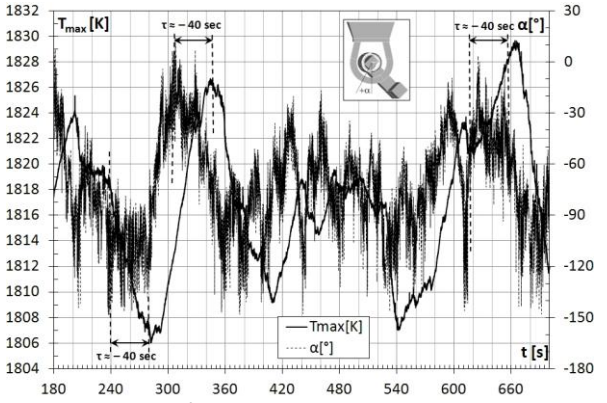

(a) – for ICF model (a), listed in Table 1

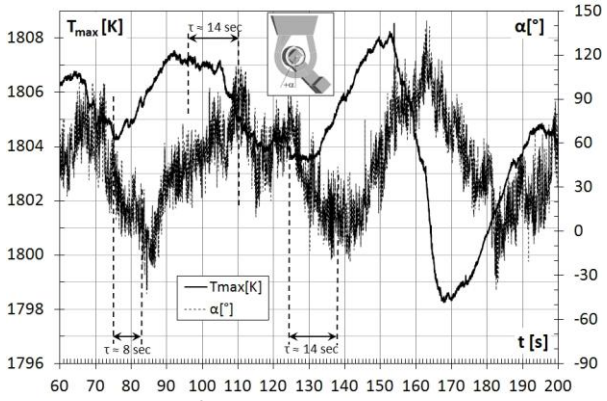

(b) for model (b), listed in Table 1

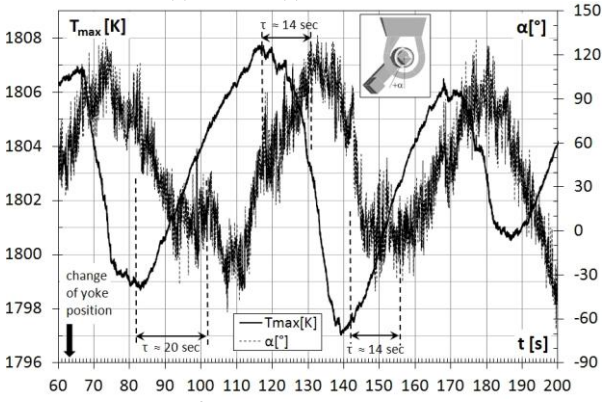

(c) for model (c), listed in Table 1

Fig. 1. Maximum temperature T_{max} and angle α of its position in ICF channel as function of flow time t

√ the main periods of oscillations of T_{max} and α are equal $t_{oscil}^{T_{max}} \sim t_{oscil}^{\alpha} \sim 55$ sec for both models;

√ typical time delays between extremes of T_{max} position α and T_{max} itself are equal $\tau \sim 14$ sec for both models for the flow time interval after 90–100 sec;

√ time-averaged temperature T_{max}^{aver} ~1803 K for model (c) is slightly less than time-averaged temperature T_{max}^{aver} ~1805 K for model (b), thus ICF construction with moved yoke provides the smaller overheating temperature;

√ deviations of temperature during oscillations for models (b),(c) are very close – compare ±5.2 K ±5.4 K, but long-term pulsations for model (c) have a more regular amplitude.

The main differences in parameters of oscillations for symmetrical (a) and asymmetrical (b), (c) models are the following:

√ the main periods of oscillations $t_{oscil}^{T_{max}}$ and t_{oscil}^{α} are greater approximately 3 times – compare ~163 sec and ~55 sec;

√ time delay between extremes of T_{max} position α and T_{max} itself is greater approximately 3 times too – compare ~40 sec and ~14 sec.

√ in contrast to models (b), (c) the extreme of T_{max} lags the extreme of T_{max} position α.

The values of time-averaged transit velocity v_{trans} for models (b), (c) are very close –3.1 and –3.3 cm/s. Transit velocity is directed to the widened (left) channel branch, which is the region with better conditions for development of thermal-gravitational convection. Thus it is the stronger factor, which enforces the T_{max} to remain in the widened channel branch, if compare with the influence of EM sources' maxima position.

For model (a) the only non-symmetrical factor is EM sources' maxima position. Therefore transit velocity is directed to channel branch with EM sources' maxima

position – v_{trans} ~ 2.6 cm/s.

3 Influence of ICF Clogging on Velocity and Temperature Field

The main properties and distributions of Joule heat power, temperature field and melt flow for models (d), (e),(f) with clogging are show in **Fig. 2, 3** and Tab. 2.

The ***Joule heat power*** distributions in the lower part of the channel loop, i.e., relatively far from clogging zones, are similar for all models. The concentration of Joule heat are obtained for model (e) (cross-section x=0 in Fig. 3(b)) at the bottom of the interface of sediments and slant surface of throat as well as in narrowed channel branch for model (d) (cross-section y=0 in Fig. 2(a)). The greatest integral value of Joule heat power in the melt 250 kW (Tab. 2) is for the model (e). Thus the clogging may be a cause of noticeable concentration of Joule heat power in zones near sediments and thus may be a reason for re-distribution of integral Joule heat power between various ICF zones.

The positions of ***temperature*** maximum for models (d), (e), (f) tend to be found in the right channel branch (see Fig. 2 (b), Fig. 3 (c)) – opposite to position of Joule heat maximum in the left channel branch, which corresponds to position of inductor's iron yoke. It may be explained by transit velocity direction to the right channel branch (Tab. 2), which is obtained by *k-ω* SST model. The previous experience [1-3] shows that during long-term computations with LES approach the results may substantially change.

The value of temperature maxima for models (e), (f) (Tab. 2) shows that non-conductive sediments at the throat bottom may be a cause of noticeable local overheating of melt for fixed inductor current, which may shorten the effective operation period of industrial ICF.

The ***velocity*** distributions in channel loop are similar – see, for example, Fig. 2 (c), where for cross-section y = 0 the perpendicular component v_y is shown. Maximal values of velocity are very close (Tab. 2) for models (d), (e), (f). It is clear because there are no changes of geometry in the considered element of ICF construction.

The flow patterns above clogging zones in the throat (Figure 3(d)) are similar to the flow patterns above the channel outlets for models (a), (b) without sediments with characteristic four contours of circulation [1].

The comparison of computationally obtained (Fig. 2(c), Fig, 3(d)) and experimentally measured [4] velocity vectors show qualitative similarity of flow patterns.

Table 2 Velocity and thermal field properties for various ICF models, listed in Table 1

ICF models, listed in Table 1			**(a)**		**(b)**		**(c)**		**(d)**		**(e)**		**(f)**	
Maximum velocity v_{max}			1.4 m/s at t ~ 660 s		3.1 m/s at t ~ 153 s		3.2 m/s at t ~ 117 s		2.2 m/s		2.1 m/s		2.0 m/s	
(Averaged) transit velocity v_{trans}			2.6 cm/s for t = 290–700 s		-3.1 cm/s for t = 65–195 s		-3.3 cm/s for t = 65–195 s		6.8 cm/s		2.2 cm/s		14.1 cm/s	
T_{max} and α oscillation periods $t_{oscil}^{T_{max}}$ and t_{oscil}^{α} *(FFT analysis)*			~ 163 s for t = 380–700 s		~ 55 s for t = 65–175 s		~ 55 s for t = 65–175 s		–		–		–	
Time delay τ between extremes of T_{max} position α and T_{max}			~ –40 s **T_{max} lags α**		~ 14 s **α lags T_{max}**		~ 14 s **α lags T_{max}**		–		–		–	
Total Joule heat power			215 kW		215 kW		215 kW		223 kW		250 kW		238 kW	
Maximum temperature T_{max}			1830K at t ~ 660 s		1809K at t ~ 153 s		1808K at t ~ 117 s		1812K		1878K		1841K	
Boundary surfaces	**Boundary conditions**		**Thermal power losses through boundary surfaces**											
	k [W/m²·K]	T_{ext} [K]	[kW]	[%]	[kW]	[%]	[kW]	[%]	[kW]	[%]	[kW]	[%]	[kW]	[%]
Bath – *convection (k and T_{ext} values in brackets are for model (a))*														
– top – *radiation*	*ε = 0.14 (0.15)*	*1650 (1600)*	-62.6	29.5%	-53.4	25.4%	-53.4	25.4%	-66.0	29.7%	-85.9	34.4%	-80.4	33.8%
– side	3 (6)	330	-43.1	20.3%	-44.5	21.1%	-44.5	21.1%	-44.4	20.0%	-45.5	18.2%	-45.2	19.0%
– bottom	7 (6)	330	-18.5	8.7%	-28.3	13.4%	-28.3	13.4%	-28.3	12.8%	-29.0	11.6%	-28.8	12.1%
Throat – *convection*														
– side	30 (6)	330	-36.2	17.0%	-34.7	16.5%	-34.7	16.5%	-34.7	15.7%	-41.7	16.7%	-37.6	15.8%
– bottom	37 (60)	330	-5.6	2.7%	-3.9	1.8%	-3.9	1.8%	-5.5	2.5%	-1.9	0.8%	-0.8	0.3%
Channel – *convection*														
– loop	33 (6)	330	-46.4	21.8%	-45.5	21.7%	-45.6	21.7%	-43.0	19.4%	-45.3	18.2%	-44.7	18.8%
Total [kW]			**-212.3**	**100%**	**-210.3**	**100%**	**-210.3**	**100%**	**-221.9**	**100.0%**	**-249.4**	**100.0%**	**-237.4**	**100.0%**

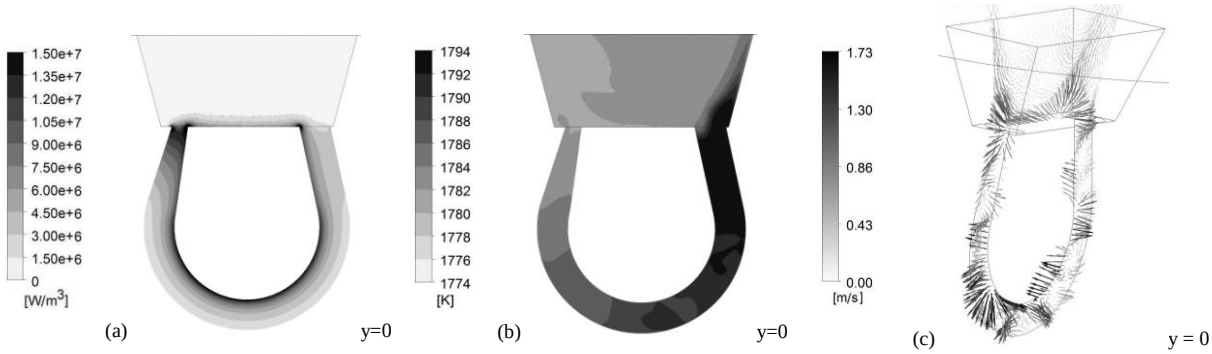

Fig. 2 Joule heat power (a), temperature field (b), velocity vectors (c) for cross-sections of Model (d) in Table 1

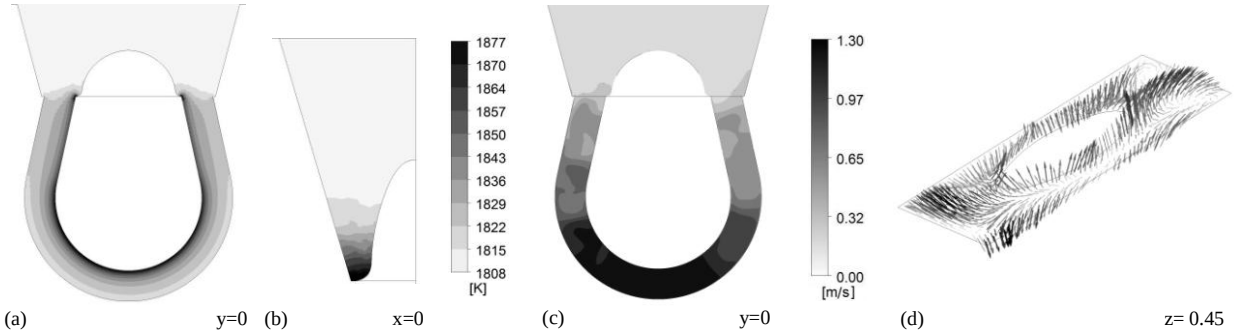

Fig. 3 Joule heat power (a, b), temperature field (c), velocity vectors (d) for cross-sections of Model (e) in Table 1

With k-ω SST model it is possible to resolve relatively large vortex structures – e.g. Fig. 2 (c) represents typical structure with angular period ~20º. To resolve more detailed turbulent structure, which may essentially contribute to heat exchange intensification along channel axis, it is necessary to use LES model of turbulence.

4 Conclusions

Long-term computations with LES approach show that relatively small ICF construction changes (channel geometry and/or iron yoke position) may be of a remarkable influence on heat and mass exchanges in the melt.

The presented qualitative estimations and results for integral hydrodynamics and thermal parameters in an industrial ICF with clogging zones in channel and at throat bottom, obtained with k-ω SST model, demonstrate the necessity of further study with substantially resource-consuming LES approach.

The computations for industrial ICF with sediments in the combination with presented experience in long-term LES analysis of melt flow and thermal field, which is supplemented with particle transport modelling [3], will stimulate the better understanding of clogging mechanisms.

References:

[1] Baake E., Jakovics A., Pavlovs S., Kirpo M. Long-term computations of turbulent flow and temperature field in the induction channel furnace with various channel design. Magnetohydrodynamics, 2010, 46 (4): 317–330.

[2] Baake E., Jakovics A., Pavlovs S., Kirpo M. Influence of channel design on heat and mass exchange of induction channel furnace. COMPEL, 2011, 30 (5): 1637–1650.

[3] Pavlovs S., Jakovics A., Baake E., Nacke B., Kirpo M. LES modelling of turbulent flow, heat exchange and particles transport in industrial induction channel furnaces. Magnetohydrodynamics, 2011, 47 (4): 399–412.

[4] Eggers A. Untersuchungen der Schmelzenströmung und des Wärmetransports im Induktions-Rinnenofen. Düsseldorf: Fortschritt-Berichte VDI, 1993.

Foundation item: financial support of European Social Fund (ESF), contract No. 2009/0223/1DP/1.1.1.2.0/09/APIA/VIAA/008.

Biography: JAKOVICS Andris (1950), male, the University of Latvia, Dr. Phys, **e-mail:** andris.jakovics@lu.lv.